The effect of carbon distribution on the manganese magnetic moment in bcc Fe–Mn alloy

2011 J. Phys.: Condens. Matter 23 326003

(http://iopscience.iop.org/0953-8984/23/32/326003)

J. Phys.: Condens. Matter **23** (2011) 326003 (5pp) doi:10.1088/0953-8984/23/32/326003

The effect of carbon distribution on the manganese magnetic moment in bcc Fe–Mn alloy

N I Medvedeva[1,2], D C Van Aken[2] and J E Medvedeva[2]

[1] Institute of Solid State Chemistry, Ekaterinburg, 620990, Russia
[2] Missouri University of Science and Technology, Rolla, MO 65409, USA

Received 2 June 2011, in final form 7 July 2011
Published 27 July 2011
Online at stacks.iop.org/JPhysCM/23/326003

Abstract
First-principles calculations were performed to study the structural, electronic, and magnetic properties of bcc Fe with C impurities alloyed with 2, 3, and 6 at.% of Mn. Our results reveal that both manganese concentration and carbon location with respect to Mn affect the Fe–Mn magnetic interaction. With an increase in Mn concentration in bcc Fe–Mn alloy, the local magnetic moment of manganese changes sharply from -2 to 1 μ_B near 3 at.% Mn, while carbon stabilizes the local ferromagnetic interaction between the nearest Mn atom and the Fe matrix. We demonstrate that the Mn–C interaction is attractive and promotes carbon trapping with a low energy defect configuration. Our results indicate that the Mn–C binding energy strongly depends on the magnetism and the formation of Mn_xC clusters is predicted.

1. Introduction

The interaction between solute and interstitial atoms plays an important role in the mechanical properties of alloys. The segregation of carbon-near manganese and the formation of Mn–C clusters are believed to affect dislocation movement and work hardening rates, and retard phase transformations in Fe–Mn–C alloys [1]. Early work assuming isotropic elasticity hypothesized that carbon would occupy the next nearest neighboring interstitial octahedral position [2]. Nuclear magnetic resonance (NMR) experiments also indicated a direct interaction between Mn and C atoms [3]. Important information on the interaction between substitutional and interstitial atoms is obtained by studying the Snoek relaxation effect, which is related to the stress-induced movement of interstitial impurities in bcc Fe [4]. It has been shown that the Snoek effect was reduced in Fe–C alloys by the addition of Mn and the formation of Mn–C dipoles was hypothesized to explain the observed decrease [5–7]. Manganese creates a strongly strained region where carbon makes no contribution in the Snoek peak. Using measurements of thermoelectric power and internal friction, it was proposed that two populations of carbon atoms existed in Fe–Mn–C alloys: free carbon and carbon trapped by manganese [8].

For carbon-free Fe_xMn_{1-x} alloys the phase stability and magnetism are well studied and a strong sensitivity to manganese concentration has been established. The ferromagnetic (FM) bcc (α) structure is stable for the manganese content below 10%, and a transformation to antiferromagnetic (AFM) fcc (γ) [9] or hcp (ε) phases according to a recent phase diagram [10] occurs for $0.75 < x < 0.9$. *Ab initio* calculations also predict an FM bcc ground state for the Fe–Mn alloys containing more than 80% Fe [11, 12]; however, the experimental [13–16] and theoretical data [12, 17–21] for the magnetic moment of manganese are contradictory, where both AFM and FM Fe–Mn coupling have been reported. Experiments on magnetic behavior in Fe–Mn alloys showed a positive magnetic moment on the Mn atom of 0.7 μ_B [13], 1.0 μ_B [14] and 0.77 μ_B [15] for 2–5 at.% Mn, whereas a negative Mn moment was observed to change sharply from -0.82 to -0.23 μ_B when the Mn content was changed from 0.8 to 1.8 at.% [16]. Controversial results were also obtained from calculations of Mn impurity in dilute Fe alloy (-1.7 μ_B [17], 0.7 μ_B [18]) and the magnetic Fe–Mn interaction was shown [18] to be close to the transition from FM to AFM coupling. Indeed, two stable configurations with antiparallel and parallel manganese magnetic moments (-2.3 and 1.6 μ_B) relative to the Fe atoms were found to have similar total energies. It was proposed that fluctuations between these quasi-degenerate states explained the contradictory observations [19]. Calculations within the tight binding, linear muffin-tin orbital (TB-LMTO)

Table 1. Lattice parameters a and c/a, the Fe–C and Mn–C distances in the [FeMn]6C octahedron, the local magnetic moment of manganese, m(Mn), and the mean magnetization M in Fe–Mn–C.

	Fe15Mn 6 at.% Mn	Fe31Mn 3 at.% Mn	Fe54Mn 1.8 at.% Mn	Fe16C	Fe15MnC 6 at.% Mn	Fe31MnC 3 at.% Mn	Fe53MnC 1.8 at.% Mn
a (Å)	2.84	2.84	2.84	2.81	2.81	2.82	2.83
c/a	1.00	1.00	1.00	1.08	1.08	1.04	1.02
$R_{\mathrm{FeI-C}}$ (Å)	—	—	—	1.80	1.80	1.79	1.79
$R_{\mathrm{FeII-C}}$ (Å)	—	—	—	1.97	1.97	1.98	1.98
$R_{\mathrm{Mn-C}}$ (Å)	—	—	—	—	1.80	1.79	1.79
m(Mn) (μ_{B})	1.03	0.99 (−1.90)	−2.20	—	1.12	0.95	0.63
M (μ_{B})	2.09	2.12	2.20	2.31	2.24	2.19	2.22

method [20] predicted a variation of the Mn moment from −2.5 to −3.0 μ_{B} with an increase in the Mn content from 5 to 20 at.%, whereas calculations for dilute Fe–Mn alloys using the coherent potential approximation to the Korringa–Kohn–Rostoker (KKR-CPA) method [12] showed a continuous variation with the concentration from −2.2 μ_{B} (1 at.% Mn) to 0.9 μ_{B} (40 at.% Mn) with a magnetic reorientation at approximately 12 at.% Mn. A strong concentration dependence of the Mn magnetic moment was also obtained within TB-LMTO calculations [21], where the Mn moment linearly changed from a large negative value −1.5 μ_{B} to a small positive value 0.5 μ_{B} at 5 at.% Mn. The equal numbers of Mn atoms with opposite directions of the magnetic moment was suggested for 2 at.% Mn, while for higher manganese concentrations, 8 at.% $< x <$ 50 at.%, the Mn moment is almost constant at approximately 1.0 μ_{B} and the magnetization of the bcc Fe–Mn alloy followed a Slater–Pauling curve [21].

Unlike for the Fe–Mn alloys, little information is available for the magnetic behavior in Fe–Mn–C alloys. Recent *ab initio* calculations [22, 23] demonstrated that the local magnetic order in austenitic Fe–C and Fe–Mn–C is strongly affected by carbon, which favors FM coupling of the nearest atoms. To our knowledge, estimations of the Mn–C binding energy in ferritic Fe–Mn–C alloys were limited to the molecular dynamic simulations [6–8]. All previous simulations were nonmagnetic and the carbon effect on the local magnetic ordering in Fe–Mn–C solutions was not established, although the crucial role of magnetism in impurity solubility and phase stability as well as in the properties of iron and iron based alloys is well known [24].

In this paper we present the results of first-principles investigations of the carbon and manganese effects on the structural, electronic, and magnetic properties of bcc Fe. The main purpose of this study is to determine how the concentration and distribution of these impurities affect the magnetic Fe–Mn coupling as well as to estimate the Fe–Mn binding energy.

2. The method

We employed the Vienna *ab initio* simulation package (VASP) in the projector augmented waves (PAW) formalism [25, 26] and used the generalized gradient approximation (GGA) introduced by Perdew, Burke, and Ernzerhof (PBE) [27] for the exchange–correlation functional. Our calculations were carried out using a kinetic energy cutoff of 350 eV for the expansion of valence orbitals in the plane waves and a k-point sampling grid that were sufficient for the total energy calculations with a convergence better than 0.01 eV/atom. The simulation of $Fe_{1-x}Mn_xC_y$ alloys was performed using Fe15MnC, Fe31MnC and Fe53MnC supercells, which correspond to Mn and C concentrations of about 6%, 3%, and 1.8%, respectively. Carbon was inserted in the interstitial octahedral site, which was previously shown to be energetically more favorable than the tetrahedral location [28]. Manganese was substituted for iron. In order to establish the role of carbon, we compared the results for the $Fe_{1-x}Mn_xC$ supercells with carbon-free supercells (Fe15Mn, Fe31Mn and Fe53Mn) and considered different site locations of carbon with respect to Mn in the Fe53MnC supercell. All of the calculations were spin-polarized and the equilibrium relaxed geometry (lattice parameters and atomic positions) was determined via the total energy and minimization of atomic forces.

3. Results and discussion

First, for bcc Fe, we find the lattice parameter and the magnetic moment to be 2.836 Å and 2.21 μ_{B}, respectively. These results were in good agreement with previous FLAPW (full potential linearized augmented plane wave) results showing 2.84 Å and 2.20 μ_{B} [29]. Our results for ferromagnetic $Fe_{1-x}Mn_xC_y$ are shown in table 1. The local magnetic moment of manganese in bcc $Fe_{1-x}Mn_x$ strongly depends on the Mn concentration and changes from the large negative value of −2.20 μ_{B} at 1.8 at.% Mn to the positive value of 0.99 μ_{B} at $x = 3$ at.% Mn. We obtained two stable quasi-degenerate states with parallel and antiparallel (reported in parentheses) directions of the magnetic moment for the 3 at.% Mn alloy. Thus, our results are in accord with the previous calculations [5, 21] where the manganese moment was found to change sharply from −2 μ_{B} to the almost constant value of 1.0 μ_{B} at a concentration between 2 and 3 at.% Mn for the bcc $Fe_{1-x}Mn_x$ alloys.

Interstitial carbon inserted in the octahedral position results in a strong relaxation of the nearest iron atoms and produces a tetragonal distortion of the bcc lattice (see table 1 and [28]). In Fe–C alloys the carbon would have two apical (FeI) and four planar (FeII) nearest neighbors at the distances of 1.42 Å and 2.00 Å, respectively. For Fe15C, the relaxation decreases the distortion of the CFe6 octahedron and the apical FeI–C distance increases to 1.80 Å, while

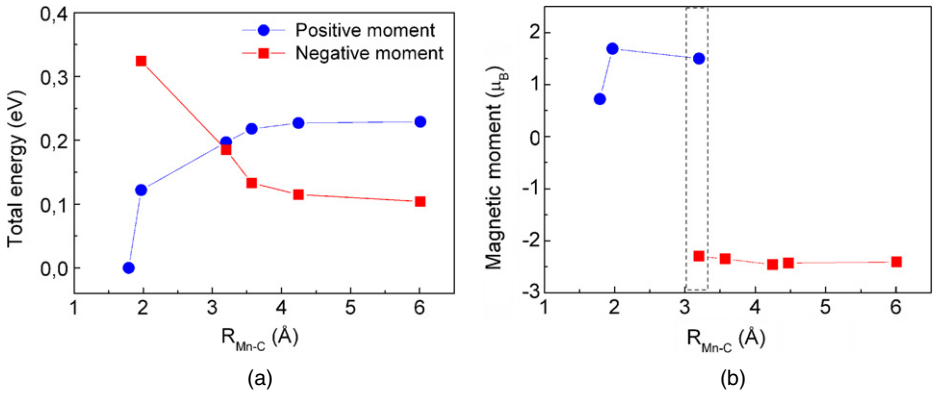

Figure 1. (a) Total energies for positive and negative Mn magnetic moments and (b) the local magnetic moment of manganese for the lowest energy states versus the Mn–C distance in Fe–1.8 at.% Mn–C. The lowest total energy was taken as zero.
(This figure is in colour only in the electronic version)

the FeII–C distances are almost unchanged at a distance of 1.97 Å. The FeI–C and FeII–C distances were not found to be dependent upon supercell size as shown in table 1. Previous cluster calculations [30] also showed a large relaxation near carbon, but predicted outward shifts for both the FeI and FeII atoms by 0.46 Å and 0.11 Å, respectively. Comparing the total magnetization for the Fe–C and Fe–Mn phases, we find that carbon and manganese have opposite effects on the ferromagnetism in bcc Fe (table 1), by increasing and reducing it, respectively. In the Fe–C solid solution, carbon increases magnetization due to a larger volume and Fe 3d–C 2p hybridization, while manganese, being an AFM metal, favors the FM–AFM transformation in the Fe–Mn alloy.

No evident changes were obtained for the lattice parameter a or the tetragonality c/a in Fe–C with the addition of manganese. In the Fe6C octahedron, it is favorable for manganese to substitute for one of the FeI atoms, and the Mn and FeI atoms are located at equal distances from the carbon. We find that manganese has FM coupling with the Fe atoms in [FeMn]6C for all of the Mn concentrations considered. For the Mn and C concentrations of 6 and 3 at.% (Fe15MnC and Fe31MnC), the Mn magnetic moment is the same as it is without carbon (table 1). However, for $x = 3$ at.% (Fe31MnC), we obtained only one stable magnetic state with a positive moment for manganese. This is in contrast to the case for bcc Fe31Mn, where two stable states with opposite magnetic moments for manganese were found. At a lower Mn content, the magnetic moment of the manganese atom located near carbon decreased, but it does not change the orientation of the magnetic moment and remains ferromagnetically coupled with the Fe. For Fe53MnC, the manganese moment is 0.63 μ_B, while it is equal to -2.20 μ_B without the carbon impurity (Fe53Mn). Thus, our results demonstrate a competition between the FM and AFM couplings of Fe and Mn in alloys with Mn concentration between 2 and 3 at.%, while carbon stabilizes the FM interaction between the nearest Mn atom and the Fe atoms in Fe–Mn–C alloys. Ferromagnetically ordered clusters with the carbon atom were also predicted in AFM fcc Fe–C and Fe–Mn–C alloys [22, 23]. In fcc Fe–C, an increase in the carbon concentration induces instability of the AFM state relative to the FM state and the AFM–FM transition takes place at 10 at.% C [24]. The mechanism of the carbon effect on the local magnetic order, both in bcc and in fcc Fe alloys, is closely associated with the volume expansion induced by the occupation of interstitial sites.

To predict whether the distribution of manganese and carbon is completely random or manganese may scavenge carbon, we compared the total energies, E_{tot}, for different octahedral interstitial positions of carbon relative to the substitutional manganese atom in Fe53MnC. Our calculations show a nonlinear dependence of the total energy and magnetic moment of manganese on the Mn–C distance, R_{Mn-C} (figure 1). We find that the nearest octahedral interstitial location relative to the substitutional manganese atom (FeI site) has the lowest energy (figure 1(a)). Manganese substituted for FeII atoms ($R_{Mn-C} \approx 2$ Å) in the [FeMn]6C octahedron or located in the second-neighbor site ($R_{Mn-C} \approx 3$ Å) has twice the magnetic moment and the total energy is 0.15–0.20 eV higher. For $R_{Mn-C} \approx 3$ Å, the total energies of configurations with positive (1.6 μ_B) and negative (-2.3 μ_B) manganese magnetic moments have similar energies (this region is denoted by dashed lines in figure 1(b)). Among the lowest energy states, we find that manganese has a positive magnetic moment when $R_{Mn-C} \leqslant 3$ Å (figure 1(b)), but a further increase in the Mn–C distance leads to a sharp parallel to antiparallel reorientation of the Mn moment. When the distance between carbon and manganese atoms is larger than 3.5 Å, manganese has a constant negative moment of about -2 μ_B, and the curve corresponding to ferromagnetic Fe–Mn coupling is higher in energy by approximately 0.1 eV for R_{Mn-C} greater than 4 Å (figure 1(a)).

In accordance with previous findings [16–18], the orientation of the impurity magnetic moment is mainly determined by how the impurity 3d states hybridize with majority- and minority-spin subbands of iron. Note that each of these subbands, as it is typical for bcc transition metal, consists of two groups of peaks with a minimum in between. Early 3d impurities (V, Cr) couple more strongly to shallow minority-spin Fe subbands, yielding an inverse local moment. For further impurities with deeper 3d energies,

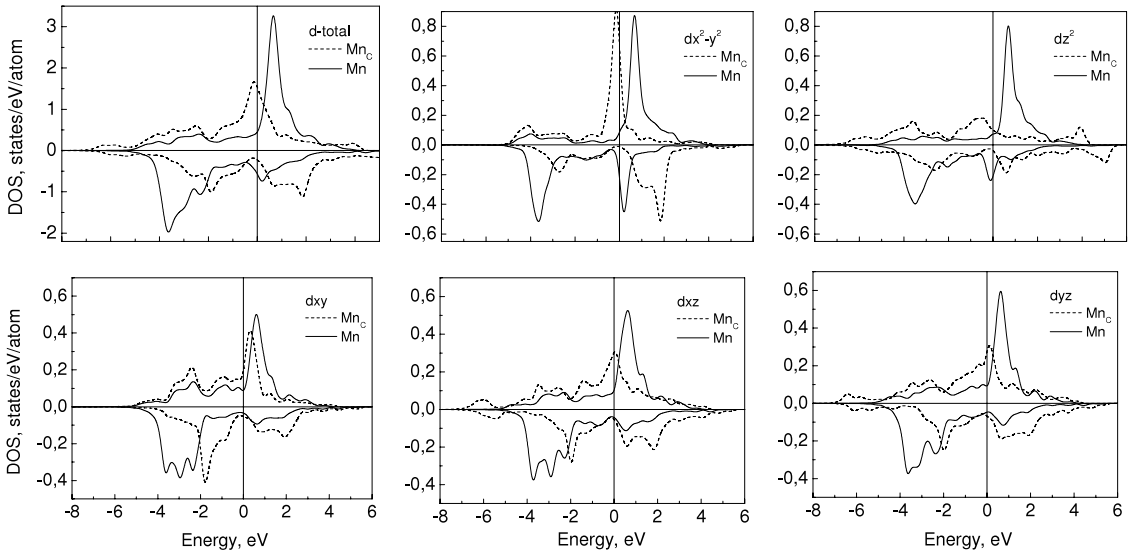

Figure 2. The local densities of d states of carbon-near (Mn_C) and carbon-distant (Mn) manganese in Fe53MnC supercells.

the hybridization with broader majority-spin band gradually becomes dominating, which eventually sets the impurity spin parallel to that for the Fe bulk. For the Mn impurity, which is close to the crossover regime but apparently favors remaining antiparallel to the magnetic moment, the situation changes where a carbon atom appears as its nearest neighbor. A comparison of the local densities of states of carbon-near (Mn_C) and carbon-distant (Mn) manganese in Fe53MnC supercells (figure 2) shows the following. The most marked difference between the two cases, and affecting the orientation of the magnetic moment, is in the density of $d_{x^2-y^2}$ states (carbon-near Mn being in the z-direction), followed by d_{z^2}, very broad and flattened due to the Mn d_{z^2}–C p_z interaction. The d_{xz} and d_{yz} states, 'collaterally touching' the C p_z lobe, are only moderately affected, but they also show a slight favoring of a magnetic polarization parallel to that of the bulk. Only the d_{xy} states, lying in the plane which does not pass through carbon atoms, are relatively unaffected by the presence of C in the vicinity, and maintain an antiparallel (to that of Fe) spin orientation. An inspection of these figures leads us to suggest that the directional and short-ranged interaction the Mn 3d and C 2p states removes the reason for an impurity moment to be set antiparallel to the bulk one: rather than hybridizing with minority-spin Fe 3d states, Mn 3d states are involved in strong coupling with spin-indifferent C 2p states. The resulting hybridized states span a broad energy interval over both spin channels, and they are largely shaped, and magnetically driven, by the band structure of the host Fe.

The total energy difference between the nearest and distant positions of Mn and C atoms may be associated with the Mn–C binding energy, E_b. Our calculations for the Fe53MnC supercell give a binding energy, E_b, of approximately 0.1 eV. This result demonstrates that the interaction between the nearest Mn and C atoms is attractive and carbon is trapped by manganese. The binding energy of Mn–C dipoles estimated from experiment and atomistic modeling varies from 0.14 to 0.46 eV [8], which is larger than our predicted value of 0.1 eV.

According to our results, the Mn–C binding energy should depend on the manganese concentration. Firstly, E_b should increase with Mn concentration due to reorientation of the Mn magnetic moment. The binding energy of 0.1 eV was obtained for bcc Fe alloy with 1.8 at.% Mn, where manganese remote from the carbon has a negative magnetic moment. For higher Mn concentrations, the manganese moment is positive for all manganese–carbon configurations and the Mn–C binding energy should increase according to figure 1(a) to 0.22 eV, which gives better agreement with experiment. Secondly, the binding energy increases due to the formation of MnC clusters, where bonding may be stronger than in the two-atom Mn–C pair. Indeed, we performed calculations for close and remote positions of two manganese atoms in the Fe52Mn2C supercell and found that they favor occupation of the apical positions nearest to carbon and form a 180° Mn–C–Mn pair. In this case, the binding energy increases to 0.48 eV. Thus, the Mn–C binding energy is dependent upon the magnetism, Mn concentration, and formation of Mn_xC clusters.

4. Summary

Using *ab initio* calculations we demonstrated that the reorientation of the Mn magnetic moment in Fe–Mn–C not only occurs with increasing manganese concentration up to 2–3 at.% Mn, but also may take place locally near light interstitial impurities even at lower Mn concentrations. Interstitial carbon significantly suppresses the antiferromagnetic interaction between Fe and the Mn atom nearest to the carbon. As a result, manganese, even at a very low concentration, may show both a positive and a negative magnetic moment, depending on its substitutional site relative to the carbon, whereas there is only ferromagnetic Fe–Mn coupling for concentrations above 3 at.% Mn. Thus, we demonstrate that the Mn moment in ferritic Fe–Mn–C alloys is highly susceptible not only to Mn concentration, but also to the distribution of interstitial carbon. The local ferromagnetic ordering near carbon arises

not only in fcc Fe and fcc Fe–Mn, as was shown previously, but also in bcc Fe–Mn. We predict that the Mn–C interaction is attractive and the Mn–C binding energy depends on the Mn concentration. The Mn–C binding energy increases with the Mn concentration due to the reorientation of the Mn magnetic moment at approximately 2–3 at.% Mn and the formation of the MnC clusters.

Acknowledgments

This work was supported by the National Science Foundation (grant CMMI-0726888). NIM also acknowledges the support from the Russian Foundation for Basic Research (Grant No. 09-03-00070a). We thank Dr A Postnikov for helpful discussion.

References

[1] Lu Y P, Zhu R F, Li S T, Zhang F C and Wang S Q 1999 *Prog. Nature Sci.* **9** 539
[2] Leslie W C 1981 *The Physical Metallurgy of Steels* (New York: McGraw-Hill)
[3] Nasu S, Takano H, Fujita F E, Takanashi K, Yasuoka H and Adachi H 1986 *J. Magn. Magn. Mater.* **54–57** 943
Nasu S, Takano H, Fujita F E, Takanashi K, Yasuoka H and Adachi H 1986 *Hyperfine Interact.* **28** 1071
[4] Nowick A S and Berry B S 1972 *Anelastic Relaxation in Crystalline Solids* (New York: Academic)
[5] Saitoh H and Ushioda K 1993 *Mater. Trans. JIM* **34** 13
[6] Saitoh H, Yoshinaga N and Ushioda K 2004 *Acta Mater.* **52** 1255
[7] Numakura H, Yotsui G and Koiwa M 1995 *Acta Metall. Mater.* **43** 705
[8] Massardier V, Patezour E L, Soler M and Merlin J 2005 *Metall. Mater. Trans.* **36A** 1745 and references therein
[9] Endoh Y and Ishikawa Y 1971 *J. Phys. Soc. Japan* **30** 1614
[10] Acet M, Schneider T, Gehrmann B and Wassermann E F 1995 *J. Physique* IV **5** 379
[11] Herper H C, Hoffmann E and Entel P 1997 *J. Physique* IV **7** 71
[12] Kulikov N I and Demangeat C 1997 *Phys. Rev.* B **55** 3533
[13] Nakai Y and Kanamori N 1975 *J. Phys. Soc. Japan* **39** 1257
[14] Child H R and Cable J W 1976 *Phys. Rev.* B **13** 227
[15] Radhakrishna P and Livet F 1978 *Solid State Commun.* **25** 597
[16] Kajzar F and Parette G 1980 *Phys. Rev.* B **22** 5471
[17] Akai H, Akai M and Kanamori J 1985 *J. Phys. Soc. Japan* **54** 4257
[18] Drittler B, Stefanou N, Blugel S, Zeller R and Dederichs P H 1989 *Phys. Rev.* B **40** 8203
[19] Anisimov V I, Antropov V P, Lichtenstein A I, Gubanov V A and Postnikov A V 1988 *Phys. Rev.* B **37** 5598
[20] Ghosh S, Sanya B, Chaudhuri C B and Mookerjee A 2001 *Eur. Phys. J.* B **23** 455
[21] Mirzoev A A, Yalalov M M and Mirzaev D A 2006 *Phys. Met. Mettall.* **101** 341
[22] Boukhvalov D W, Gornostyrev Yu N, Katsnelson M I and Lichtenstein A I 2007 *Phys. Rev. Lett.* **99** 247205
[23] Medvedeva N I, Van Aken D C and Medvedeva J E 2010 *J. Phys.: Condens. Matter* **22** 316002
[24] Pepperhoff W and Acet M 2001 *Constitution and Magnetism of Iron and Its Alloys* (Berlin: Springer)
[25] Kresse G and Furthmüller J 1996 *Phys. Rev.* B **54** 11169
[26] Kresse G and Hafner J 1996 *J. Phys.: Condens. Matter* **6** 8245
[27] Perdew J P, Burke K and Ernzerhof M 1996 *Phys. Rev. Lett.* **77** 3865
[28] Jiang D E and Carter E A 2003 *Phys. Rev.* B **67** 214103
[29] Herper H C, Hoffmann E and Entel P 1999 *Phys. Rev.* B **60** 3839
[30] Hong S Y and Anderson A B 1989 *Phys. Rev.* B **40** 7508